Modeling of a biological cell exposed to an electrical pulse: a Discrete Dual Finite Volume method application

Thomas Bonnafont, Delphine Bessières, Jean Paillol

Modeling of a biological cell exposed to an electrical pulse: a Discrete Dual Finite Volume method application

Thomas Bonnafont*(1), Delphine Bessieres (2), and Jean Paillol(2)
(1) Lab-STICC UMR CNRS 6285, ENSTA Bretagne, 29200 Brest, France
(2) Laboratoire SIAME, Université de Pau & des Pays de l'Adour/E2s, 64000 Pau, France

Abstract

This article proposes a finite volume-based computational method to simulate a cell's response to an electrical pulse. The membrane of the cell and dielectric dispersion is accounted for leading to a Poisson equation with heterogeneous jump conditions. To address this, we employ a tailored discrete dual finite volume scheme, ensuring precise treatment of jump conditions and demonstrating second-order convergence. Numerical tests are provided in both the stationary a non-stationary cases to show the effectiveness of the method.

1 Introduction

The *electropermeabilization* phenomena [1] occurs when a sufficient electrical pulse is applied to a biological cell. This latter, also known as electroporation, allows to open pores in the cell's membrane either reversibly or irreversibly. The state of permeabilization depends on the *transmembrane voltage*, i.e. the difference of potentials at the inner and outer surface of the membrane. This phenomenon has multiple applications in various domains [1].

This phenomenon has been well-studied experimentally [1], and some clinical tests have been performed [1]. Nonetheless, there is a need for predictive *computational methods* to properly adapt the electric field. This modeling is challenging. First, we deal with a partial differential equation with jump conditions on irregular boundaries [2]. Second, the membrane is very thin compared to the computational domain. Finally, the conductivity of the membrane is changing with the transmembrane voltage.

Most of the computation schemes are based on the finite element method [2] or the use of the commercial software COMSOL [3]. Besides, for the electroporation different models are used, either based on the Krassowska, Neu *et al.* asymptotic equations [4], or the one developed by Leguèbe *et al.* [5]. However, in general, the membrane thickness is not accounted for and an equivalent model of the membrane is used instead. Indeed, the difference in size between the different media is a burden for finite element schemes. However, Mescia *et al.* [6] have shown that the thickness shall be accounted for.

Recently in [7], we have proposed to use a finite volume scheme, i.e., *the discrete dual finite volume method* (DDFV) [8], to accurately model a cell exposed to an electrical field. In particular, the membrane thickness is taken into account. Indeed, DDFV allows us to properly take into account jump conditions at interfaces [8]. Nonetheless, in [7] we only studied the stationary case.

The aim of this paper is to generalize our previous study [7] to the nonstationary case while accounting for dispersive species, as in [3]. To do so, the cell's model is expressed as a Poisson equation with jump conditions. The dispersive nature of the media is introduced through a 1st-order Debye model, and the model of [5] is used to account for the electroporation of the membrane. This set of equations is then solved using a tailored DDFV scheme. Numerical results are shown in both the stationary and non-stationary cases.

2 Model and notations

2.1 Quasi-static electrical model of the cell

We use here the single-shell model, where the cell is described by two subdomains, the membrane, denoted by Ω_m, and the cytoplasm, denoted by Ω_c, as illustrated in Figure 1. The exterior media is denoted as Ω_e. The interfaces between each medium are denoted by $\Gamma_{e,m}$ and $\Gamma_{m,c}$, as pictured in Figure 1. All these media have different dielectric parameters, denoted by ε_i and σ_i for their respective permittivity and conductivity.

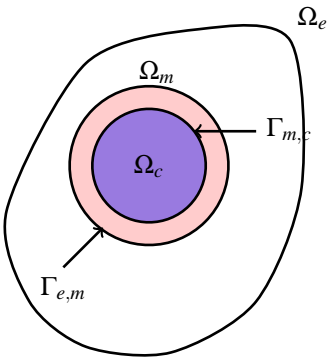

Figure 1. Single shell-model of the cell.

First, in this case, the magnetic field can be neglected, leading to a quasi-static study [3, 5, 6]. Second, since the quantity of interest here is the transmembrane voltage, denoted by U_m, and corresponding to a difference of potential, we work with the electric potential V.

The electro-quasi-static model accounting for the membrane thickness is then given as

$$\begin{cases} -\nabla\cdot\left(\varepsilon_i\frac{\partial\nabla V_i}{\partial t}+\sigma_i\nabla V_i\right) = 0 \\ \left(\varepsilon_m\frac{\partial\nabla V_m}{\partial t}+\sigma_m\nabla V_m-\varepsilon_e\frac{\partial\nabla V_e}{\partial t}+\sigma_e\nabla V_e\right)\cdot\mathbf{n}_{e,m} = 0 \\ \left(\varepsilon_c\frac{\partial\nabla V_c}{\partial t}+\sigma_c\nabla V_c-\varepsilon_m\frac{\partial\nabla V_m}{\partial t}+\sigma_m\nabla V_m\right)\cdot\mathbf{n}_{m,c} = 0 \end{cases} \quad (1)$$

In this set of equations, ε_i corresponds to $\varepsilon_0\varepsilon_{i,r}$, and $\mathbf{n_{i,j}}$ to the unit normal directed from media i to j. This latter is equivalent to the one described in [3], and comes from rewriting the Maxwell-Gauss relation on the electrical induction using the constitutive relation for linear and dielectric media. Furthermore, the second and third equations correspond to the transition between each medium. Mixed boundary conditions, Dirichlet and Neumann, at the boundary of Ω_e are also accounted for to complete the model.

To consider dispersive media, as in [3], we use a 1st-order Debye model, which leads to

$$\tau_i\frac{\partial\mathbf{P}_{i,\text{disp}}}{\partial t}+\mathbf{P}_{i,\text{disp}} = \varepsilon_0\left(\varepsilon_{i,r}-\varepsilon_{i,\infty}\right)\mathbf{E}_i, \quad (2)$$

where $\mathbf{P_{i,\text{disp}}}$ is the polarization due to dispersive species, τ_i corresponds to the relaxation time, $\varepsilon_{i,r}$ to the static permittivity, and $\varepsilon_{i,\infty}$ to the high-frequency permittivity of the medium considered.

2.2 Electroporation model

Now that the electro-quasi-static model of the cell has been described, we focus on the electroporation model. The electrical pulse induces a change in the membrane conductivity that is modeled by a non-linear law.

In this article, we rely on the *LMSP model* [5], because it allows us to accurately describe the state of the membrane, electroporated or permeabilized. In addition, with the LMPS model fewer parameters are needed and the functions describing the degree of poration and permeabilization are bounded when compared to other models such as [4], even if the method can also be used with the latter.

In our case, the latter reads as

$$\sigma_m(t,U_m) = \sigma_{m_0}+\sigma_1 X_1(t,U_m)+\sigma_2 X_2(t,U_m), \quad (3)$$

with σ_{m_0} the resting conductivity of the membrane, σ_1 and σ_2 the conductivity in the porated and permeabilized state, respectively. In this equation, the functions X_1 and X_2 describe the degree of poration and permeabilization of the cell's membrane. They are solutions of the two following ordinary differential equations (ODE)

$$\begin{array}{rcl} \frac{\partial X_1}{\partial t} & = & \frac{\beta_1(U_m)-X_1}{\tau_{ep}}, \\ \frac{\partial X_2}{\partial t} & = & \max\left(\frac{\beta_2(X_1)-X_2}{\tau_{perm}},\frac{\beta_2(X_1)-X_2}{\tau_{res}}\right), \end{array} \quad (4)$$

where τ_{ep}, τ_{perm}, and τ_{res} correspond to the characteristic times of the poration, permeabilization and resealing. Finally, the functions β_1 and β_2 are two linearized Heaviside functions defined as

$$\beta_i(\lambda) = \frac{1+\tanh\left(k_i\left(|\lambda|-T_i\right)\right)}{2}, \quad (5)$$

where k_i allows to modify the slope of the functions, and T_i is the threshold for going from 0 to 1.

3 A finite volume based computational scheme

3.1 Time discretization of the model

For better readability let us work with the model without dispersion. Indeed, all can be generalized to the dispersive case. Here, we use an explicit Euler scheme for the time derivative, which for equation (1) leads to

$$\begin{cases} -\nabla\cdot\left((\varepsilon_i+\Delta t\,\sigma_i^n)\nabla V_i^n\right) = f \\ \left((\varepsilon_m+\Delta t\,\sigma_m^n)\nabla V_m^n-(\varepsilon_e+\Delta t\,\sigma_e)\nabla V_e\right)\cdot\mathbf{n}_{e,m} = \sigma_{s,e,m} \\ \left((\varepsilon_c+\Delta t\,\sigma_c)\nabla V_c-(\varepsilon_m+\Delta t\,\sigma_m)\nabla V_m\right)\cdot\mathbf{n}_{m,c} = \sigma_{s,m,c} \end{cases} \quad (6)$$

where Δt corresponds to the time step and shall be of order ε_0, while the upper script n denotes the element at $t=n\Delta t$. In addition, f and $\sigma_{s,\cdot}$ correspond to source terms accounting for the previous computed term at $t=(n-1)\Delta t$.

Next, the two ODEs (4) are solved using also an explicit Euler scheme, leading to

$$\begin{array}{rcl} X_1^n & = & X_1^{n-1}+\Delta t\,\frac{\beta_1(U_m^n)-X_1^{n-1}}{\tau_{ep}} \\ X_2^n & = & X_2^{n-1}+\Delta t\max\left(\frac{\beta_2(X_1^n)-X_2^{n-1}}{\tau_{perm}},\frac{\beta_2(X_1^n)-X_2^{n-1}}{\tau_{res}}\right) \end{array} \quad (7)$$

For good accuracy the time step shall be lower than $\min(\tau_{ep},\tau_{perm},\tau_{res})\geq 10^{-7}$. Therefore, from the discretization of the PDE, we are limited to Δt of order ε_0.

Finally, when dispersion is taken into account, equation (2) is also solved using an explicit Euler scheme.

3.2 A DDFV based solver

We have thus to solve a Poisson equation with transition conditions at each time step. Since the jump conditions are flux ones, we choose to use a finite volume scheme.

Here, we choose to use and adapt the DDFV method [8], which is a finite volume scheme with a second-order convergence even when a highly distorted mesh is used. It also allows accounting for jump conditions, and contrary to usual finite volume schemes, we have a strong convergence of the gradient. Nonetheless, this comes at the cost of twice as many unknowns.

The computational domain is discretized as follows. First, we denote by $\mathscr{M}$ the *primal mesh*, corresponding to a non-overlapping partition of the domain Ω, with $\mathscr{K} \in \mathscr{M}$ the associated control volumes. Here, a quadrangular grid is chosen and obtained using the method of Hyman *et al.* [9] to create a mesh that follows the physics of the problem. Second, the method is based on the use of a *dual mesh*, denoted by $\mathscr{M}^*$, constructed from the primal mesh by considering the vertices of the primal mesh as the unknowns. The vertices of the dual volume $\mathscr{K}^* \in \mathscr{M}^*$ correspond to the center of the primal mesh. Finally, both grids are linked through the diamond mesh, denoted by $\mathscr{D}$. A diamond $D \in \mathscr{D}$ corresponds to the quadrangle defined by $x_\mathscr{K} x_{\mathscr{K}^*} x_\mathscr{L} x_{\mathscr{L}^*}$, corresponding to the center of the volumes $\mathscr{K}$, $\mathscr{K}^*$, $\mathscr{L}$ and $\mathscr{L}^*$, respectively, as shown in Figure 2. Next, both the discrete gradient and divergence operators can be introduced as follows. The first is defined as

$$\nabla^D V^\mathscr{T} = \frac{1}{2|D|}\left(\left(V_{x_\mathscr{L}} - V_{x_\mathscr{K}}\right)\mathbf{N}_\nu + \left(V_{x_{\mathscr{L}^*}} - V_{x_{\mathscr{K}^*}}\right)\mathbf{N}_{\nu^*}\right),$$

and the second as

$$\begin{aligned} \mathrm{div}^\mathscr{T}_\mathscr{K}\left(\xi^D\right) &= \frac{1}{|\mathscr{K}|}\sum_{\nu\in\mathscr{D}_\mathscr{K}} \xi^D\cdot\mathbf{N}_\nu, \\ \mathrm{div}^\mathscr{T}_{\mathscr{K}^*}\left(\xi^D\right) &= \frac{1}{|\mathscr{K}^*|}\sum_{\nu^*\in\mathscr{D}_{\mathscr{K}^*}} \xi^D\cdot\mathbf{N}_{\nu^*}. \end{aligned}$$

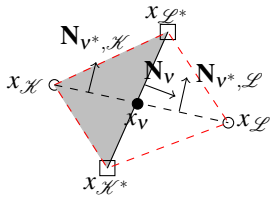

Figure 2. Illustration of a diamond D and of the corresponding half diamonds.

Next, to account for the jump conditions we use the idea of the technique derived in [8]. Nonetheless, here we have a source term σ_s in the jump condition, and we assume that the jump occurs only between primal control volumes[1]. To do so, a new unknown is added, that will be eliminated using the transition conditions as in [10], and the discretization is performed on half diamonds as shown in Figure 2. The latter are defined as

$$\begin{aligned} \nabla^{\tau_\mathscr{K}} V^\mathscr{T} &= \nabla^D V^\mathscr{T} + \frac{\delta}{|\tau_\mathscr{K}|}\mathbf{N}_\nu, \\ \nabla^{\tau_\mathscr{L}} V^\mathscr{T} &= \nabla^D V^\mathscr{T} - \frac{\delta}{|\tau_\mathscr{L}|}\mathbf{N}_\nu, \end{aligned}$$

where δ is the new unknown to be eliminated [8]. To achieve that, we use the transition condition and obtain

$$\delta = \frac{1}{|\nu|}\frac{1}{\frac{\varepsilon_\mathscr{L}}{|\tau_\mathscr{L}|}+\frac{\varepsilon_\mathscr{K}}{|\tau_\mathscr{K}|}}\left(\left(\varepsilon_\mathscr{L}-\varepsilon_\mathscr{K}\right)\nabla^D V^\mathscr{T}\cdot\mathbf{n}_\nu + \sigma_{s,\cdot,\cdot}\right),$$

[1] This is not a strict assumption since the mesh is computed to respect it using the method described in [9]

where $\sigma_{s,\cdot,\cdot}$ is the corresponding surface conductivity. It shall be noted that adding the surface conductivity only modify the right hand side.

Finally, the set of equations of (6) is discretized using the DDFV operators. This leads to

$$\begin{aligned} &\forall \mathscr{K} \in \mathscr{M},\ -\mathrm{div}^\mathscr{T}_\mathscr{K}\left(\varepsilon_\mathscr{K}\nabla^{\tau_\mathscr{K}} V^\mathscr{T}\right) = f_\mathscr{K}, \\ &\forall \mathscr{K}^* \in \mathscr{M}^*,\ -\mathrm{div}^\mathscr{T}_{\mathscr{K}^*}\left(\varepsilon_\mathscr{K}\nabla^{\tau_\mathscr{K}} V^\mathscr{T} + \varepsilon_\mathscr{L}\nabla^{\tau_\mathscr{L}} V^\mathscr{T}\right) = f_{\mathscr{K}^*}, \end{aligned}$$

where $f_\cdot$ corresponds to the source term. The system of linear equations can then be rewritten as

$$SV^\mathscr{T} = Mf^\mathscr{T} + D_\delta \sigma_s^\mathscr{T}, \tag{8}$$

where S and M correspond to the associated stiffness and mass matrix. To conclude, to account for the Dirichlet condition, we use the penalization method, while the Neumann conditions are intrinsically taken into account.

4 Numerical tests

4.1 The stationary case

We begin by studying the stationary case to show that our method is robust. The scenario is described in Figure 3, where a spherical cell is studied. The cell radius is $R_d = 0.2\ \mu$m, while the membrane thickness is $d_m = 0.0008\ \mu$m. The electrical parameters are as follows: $\varepsilon_e = \varepsilon_c = 80$, and $\varepsilon_m = 2$. We set $V^+ = 1$ V and $V^- = -1$ V at the left and ride side of the domain, respectively, and consider homogeneous Neumann conditions on the upper and lower boundaries of the domain.

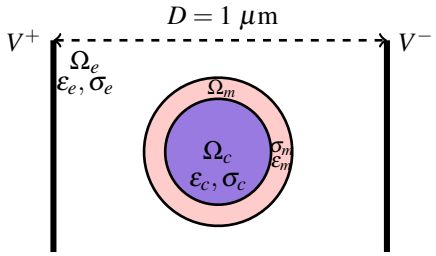

Figure 3. Numerical setup for the single spherical cell.

In Figure 4, we plot the evolution of the potential along a horizontal equatorial cut of the cell. In addition, the predicted value of the potential is also shown.

As expecgted, we observe that the potential decreases with the same slope in the exterior media and in the cell and more rapidly in the membrane (Figure 4). Furthermore, these results are in line with the analytical calculation.

4.2 Cell response to a trapezoidal pulse

Second, we study the cell response to a trapezoidal pulse. The setup is the same except that the cell's parameters are taken from [3], and that $V^- = 0$, and V^+ corresponds to the

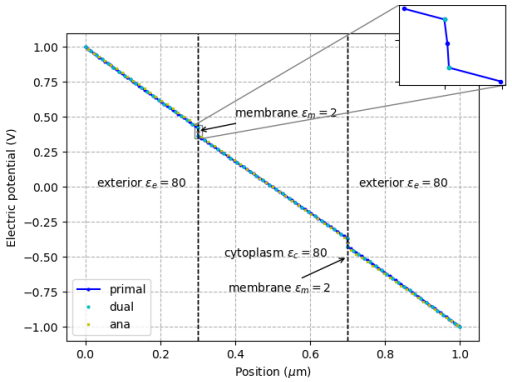

Figure 4. Potential on an equatorial cut along the cell.

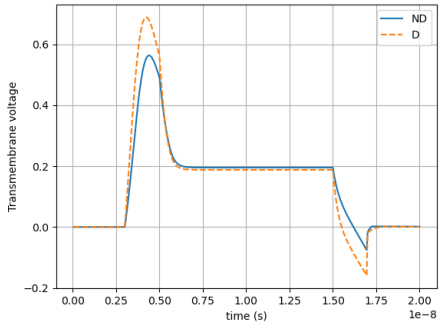

Figure 5. U_m at the pole of the cell when no dispersive (blue) or dispersive (orange) media are accounted for.

applied pulse. The computed transmembrane voltage along the pole of the cell is plotted in Figure 5.

We observe a consistent behavior: the transmembrane voltage increases with the pulse until a threshold and then decreases toward an asymptotic value. In the case of nondispersive media, we retrieve the same values and the same behavior as in [2], showing that the method works well. In the case of dispersive species, as in [3], U_m is increasing more rapidly toward a larger value. Our results are in line with the literature.

5 Conclusion

In this article, we have extended our work [7], by using and adapting the DDFV scheme to study the cell's response to an electric pulse while accounting for dispersive species.

First, as recommended in [6] the membrane is accounted for as a whole domain. The dispersive nature of the media is also introduced through a 1st order Debye model. Second, a time discretization is applied to the obtained model. For each time step, this leads to a Poisson equation with heterogeneous jump conditions. The latter is efficiently solved using a modified DDFV scheme.

Numerical experiments, conducted in both stationary and non-stationary scenarios, attest to the method's effectiveness. Further works include the study of diverse cell shape, as in [6], and of cell aggregate. We also would like to compare results with experimental studies and extend the work to the 3D case.

References

[1] T. Kotnik, W. Frey, M. Sack, S. H. Meglič, M. Peterka, and D. Miklavčič, "Electroporation-based applications in biotechnology," *Trends in biotechnology*, vol. 33, no. 8, pp. 480–488, 2015.

[2] A. Guittet, C. Poignard, and F. Gibou, "A Voronoi interface approach to cell aggregate electropermeabilization," *Journal of Computational Physics*, vol. 332, pp. 143–159, 2017.

[3] E. Salimi, D. J. Thomson, and G. E. Bridges, "Membrane dielectric dispersion in nanosecond pulsed electroporation of biological cells," *IEEE Transactions on Dielectrics and Electrical Insulation*, vol. 20, no. 4, pp. 1256–1265, 2013.

[4] J. C. Neu and W. Krassowska, "Asymptotic model of electroporation," *Physical review E*, vol. 59, no. 3, p. 3471, 1999.

[5] M. Leguebe, A. Silve, L. M. Mir, and C. Poignard, "Conducting and permeable states of cell membrane submitted to high voltage pulses: mathematical and numerical studies validated by the experiments," *Journal of theoretical biology*, vol. 360, pp. 83–94, 2014.

[6] L. Mescia, M. Chiapperino, P. Bia, C. Lamacchia, J. Gielis, and D. Caratelli, "Relevance of the cell membrane modelling for accurate analysis of the pulsed electric field-induced electroporation," in *2019 PhotonIcs & Electromagnetics Research Symposium-Spring (PIERS-Spring)*, pp. 2985–2991, IEEE, 2019.

[7] T. Bonnafont, D. Bessieres, and J. Paillol, "Finite volumes method for the cell electrical model," in *2022 3rd URSI Atlantic and Asia Pacific Radio Science Meeting (AT-AP-RASC)*, pp. 1–4, IEEE, 2022.

[8] F. Boyer and F. Hubert, "Finite Volume Method for 2D Linear and Nonlinear Elliptic Problems with Discontinuities," *SIAM Journal on Numerical Analysis*, vol. 46, pp. 3032–3070, Jan. 2008.

[9] J. M. Hyman, S. Li, P. Knupp, and M. Shashkov, "An algorithm for aligning a quadrilateral grid with internal boundaries," *Journal of Computational Physics*, vol. 163, no. 1, pp. 133–149, 2000.

[10] R. Egan and F. Gibou, "xGFM: Recovering convergence of fluxes in the ghost fluid method," *Journal of Computational Physics*, vol. 409, p. 109351, 2020.